Supporting Information

Construction of Isolated Co-N_x and Dual Co_n-CoN_x Sites for Selectivity Regulation Hydrogenation and Hydrodeoxygenation of Biomass-Derived Chemicals

Zhanghui Xia [a,b], Libo Niu [a,*], Qi Wu [a], Yadan An [a] and Guoyi Bai [a,*]

a. State Key Laboratory of New Pharmaceutical preparation and Excipients, College of Chemistry and Materials Science, Hebei University, Baoding 071002, P.R. China

b. Shanghai Key Laboratory of Green Chemistry and Chemical Processes, School of Chemistry and Molecular Engineering, East China Normal University, Shanghai 200062, P. R. China

Table of Contents

Section 1. Materials and characterization

Materials.

Cobaltous nitrate hexahydrate, isopropanol and ethanol were purchased from Tianjin Kermel Chemical Reagent Co., Ltd. 2,4-dihydroxybenzoic acid was purchased Shanghai Macklin Biochemical Co., Ltd. Hexamethylenetetramine (HMT) was purchased from Innochem Biochemical Technology Co., Ltd. Pluronic F127 was purchased from Sigma. $NH_3 \cdot H_2O$ was purchased from Tianjin Damao Chemical Reagent Factory. HMF, MFA, BHMF, MF and Melamine were purchased from Aladdin Chemistry Co., Ltd. All commercial chemicals were used without any further purification.

Catalyst characterization.

X-ray diffraction (XRD) patterns were performed on a Bruker D8 diffractometer. The inductively coupled plasma optical emission spectrometer (ICP-OES) was used to determine the Co content of all catalysts by the Agilent 730 spectrometer. Raman spectroscopy was performed on a Larbram HR Evoluction Raman system (Horiba) using in the range of 800-2000 cm^{-1} operating at 532 nm. Transmission electron microscopy (TEM) was tested on a FEI Tecnai G2 F20 microscope with an accelerating voltage of 200 kV. X-ray photoelectron spectroscopy (XPS) was recorded on a PHI 1600 equipped with Mg Kα radiation source. The ultraviolet photoelectron spectra (UPS) of all samples were recorded by PHI-5000 VersaProbe III. The XAS data of Co was collected in at 1W1B station in Beijing Synchrotron Radiation Facility. Co oxides and Co foil were employed as references for comparison. The Athena module in the FEFIT was used to analysis the acquired EXAFS data according to the standard procedures.

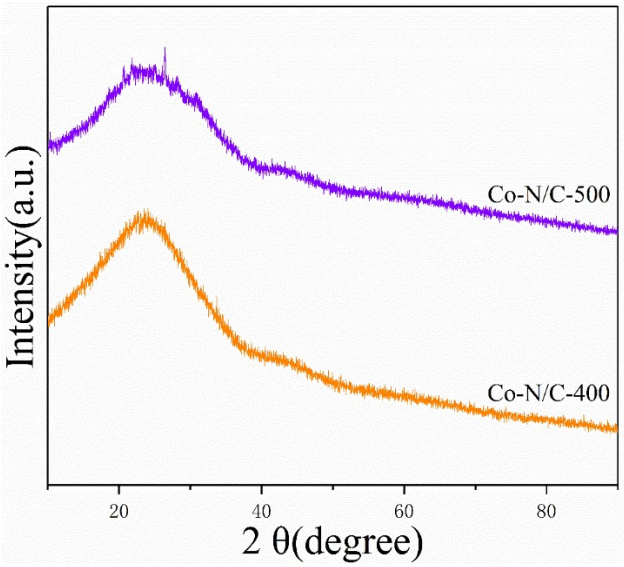

Figure S1. XRD patterns of Co-N/C-400 and Co-N/C-500.

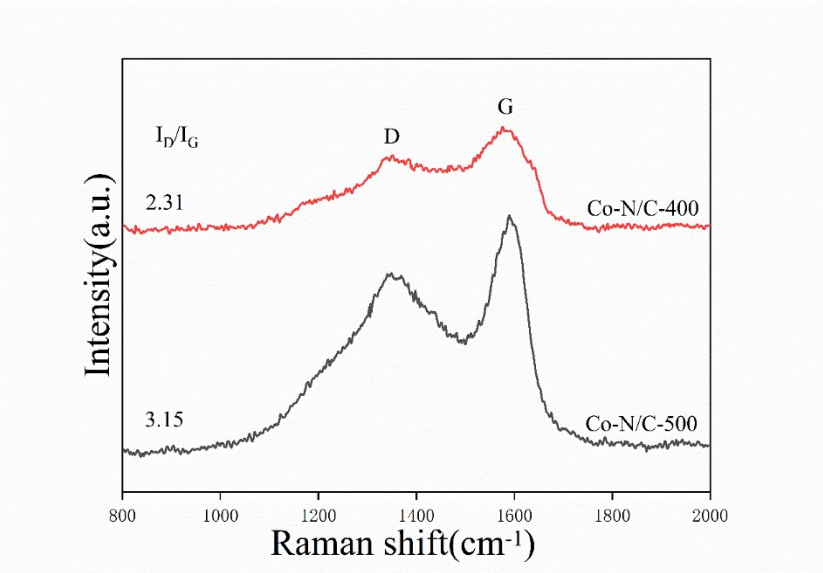

Figure S2. The Raman spectra of Co-N/C-400 and Co-N/C-500.

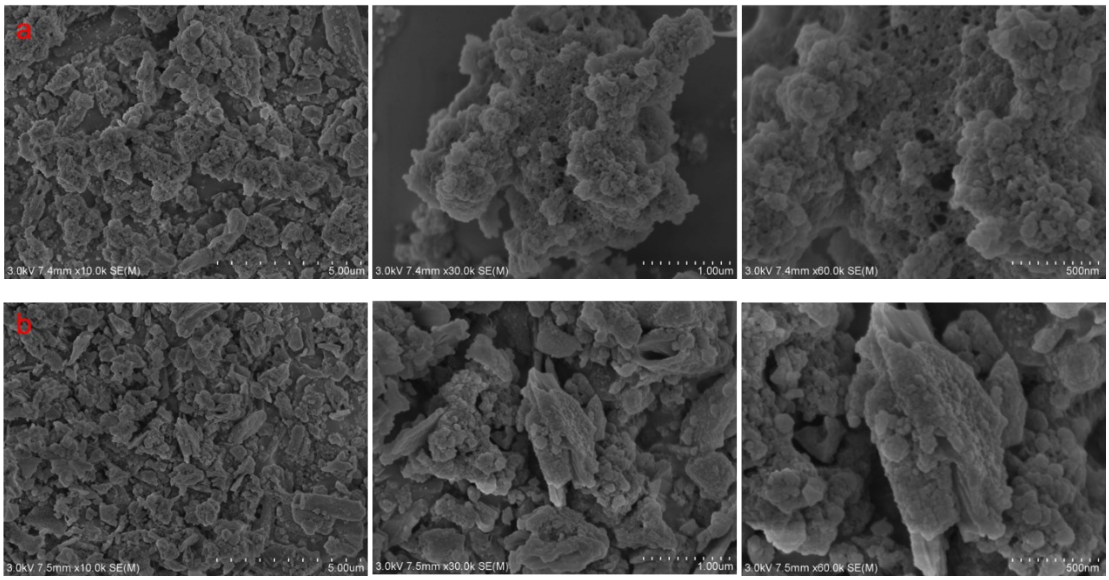

Figure S3. The SEM graphs of Co-N/C-400 (a) and Co-N/C-500 (b) samples.

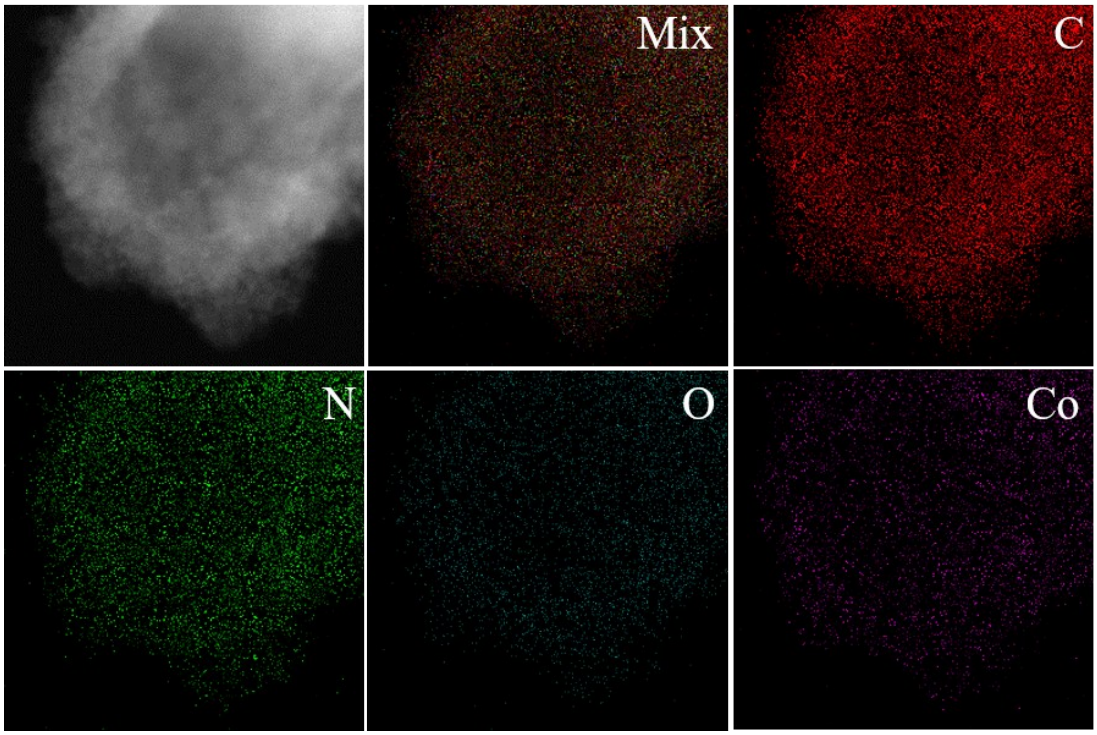

Figure S4. EDS mapping images of Co-N/C-500.

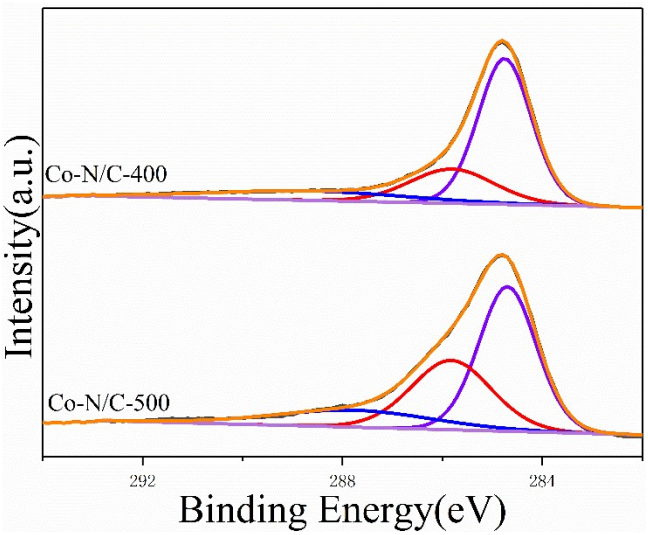

Figure S5. High-resolution of C1s spectra of Co-N/C-400 and Co-N/C-500 catalysts.

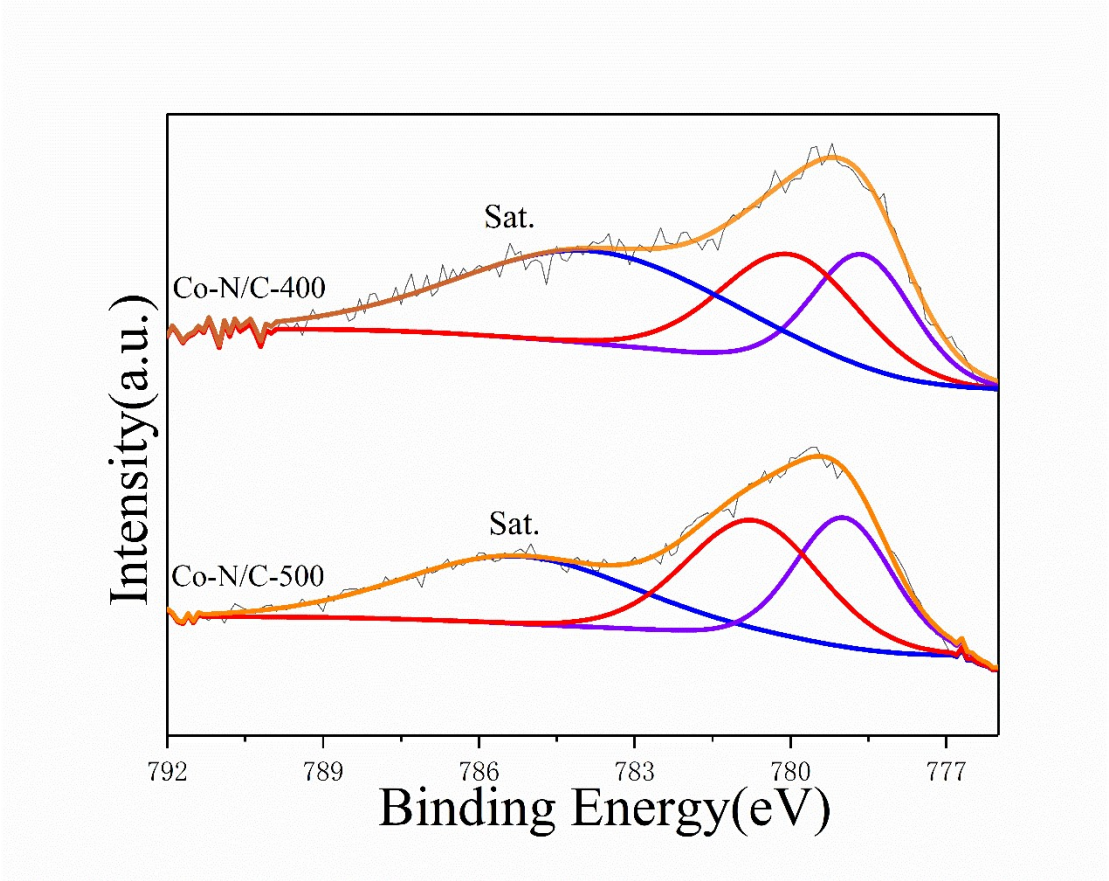

Figure S6. The XPS spectra of Co $2p_{3/2}$ of Co-N/C-400 and Co-N/C-500 catalysts.

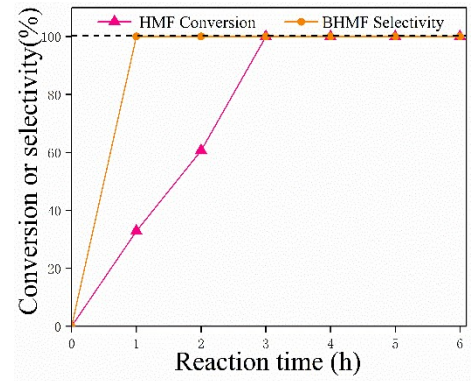

(a)

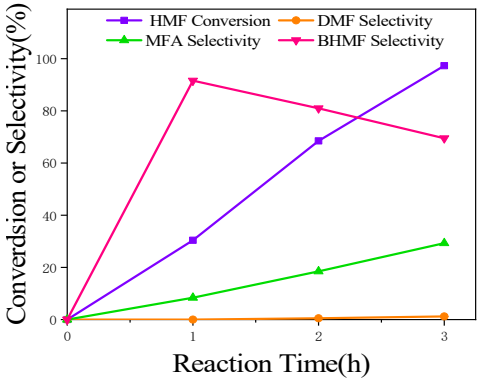

(b)

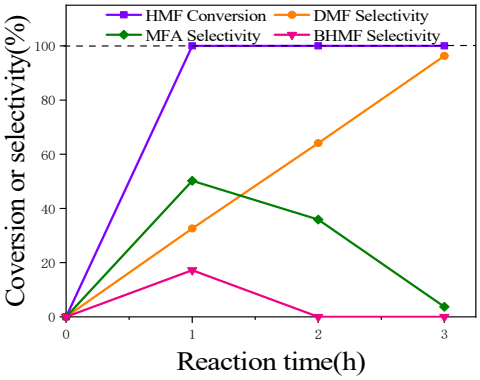

(c)

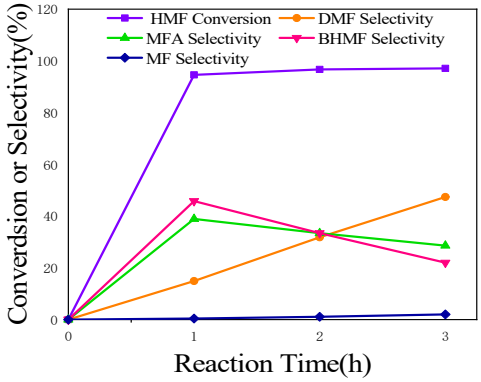

(d)

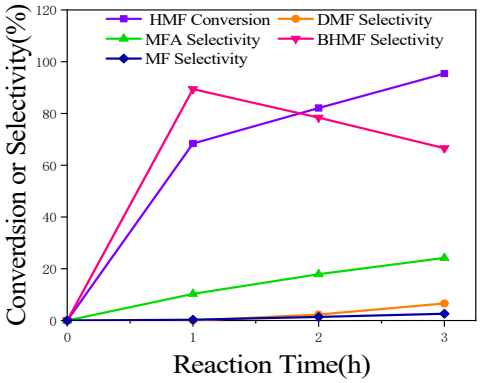

(e)

Figure S7. The HMF hydrogenation over Co-N/C-400(a), Co-N/C-450(b), Co-N/C-500(c), Co-N/C-550(d) and Co-N/C-600(e) catalysts as a function of reaction time.

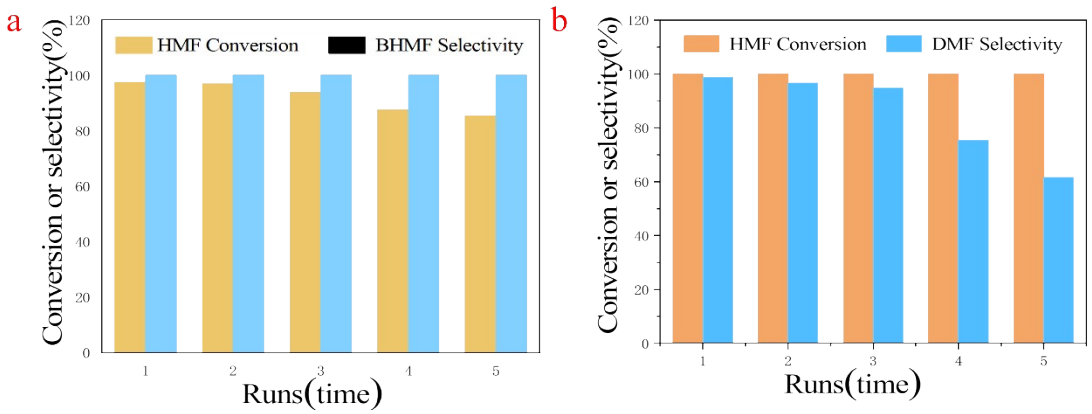

Figure S8. Catalytic stability of Co-N/C-400 (a) and Co-N/C-500 (b) samples.

Co-N/C-400

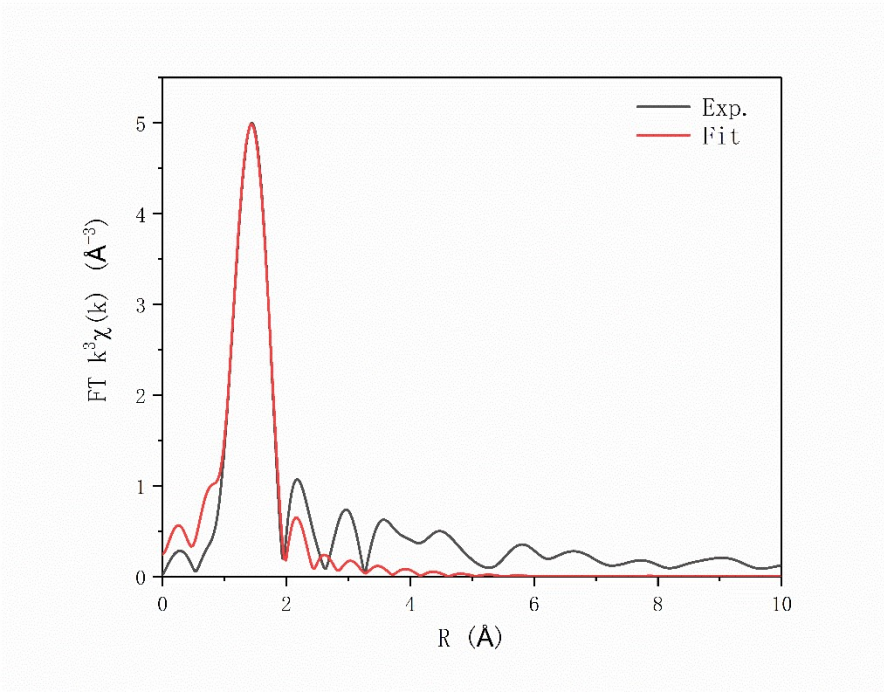

Co-N/C-500

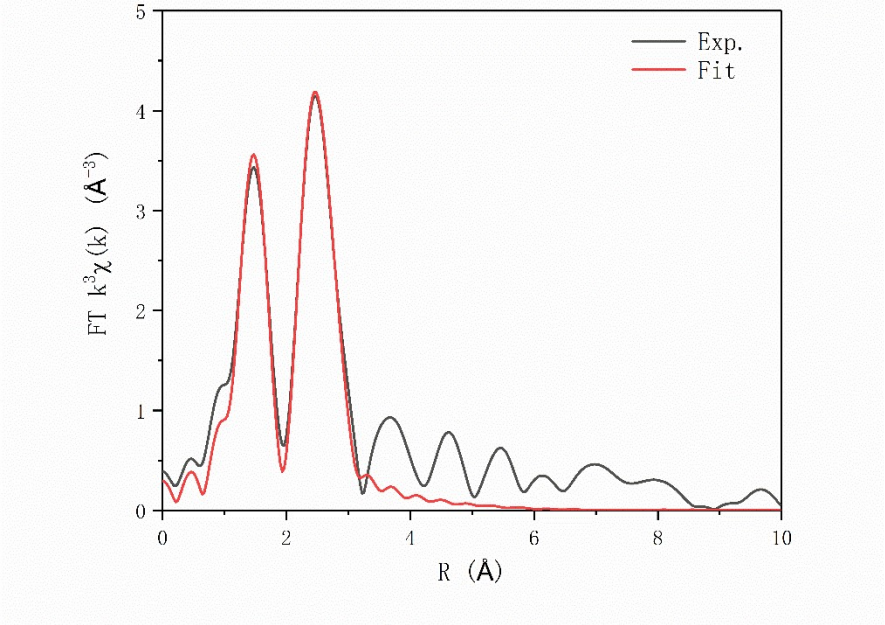

Figure S9. EXAFS spectrum fitting curves of Co-N/C-400 and Co-N/C-500 at R space.

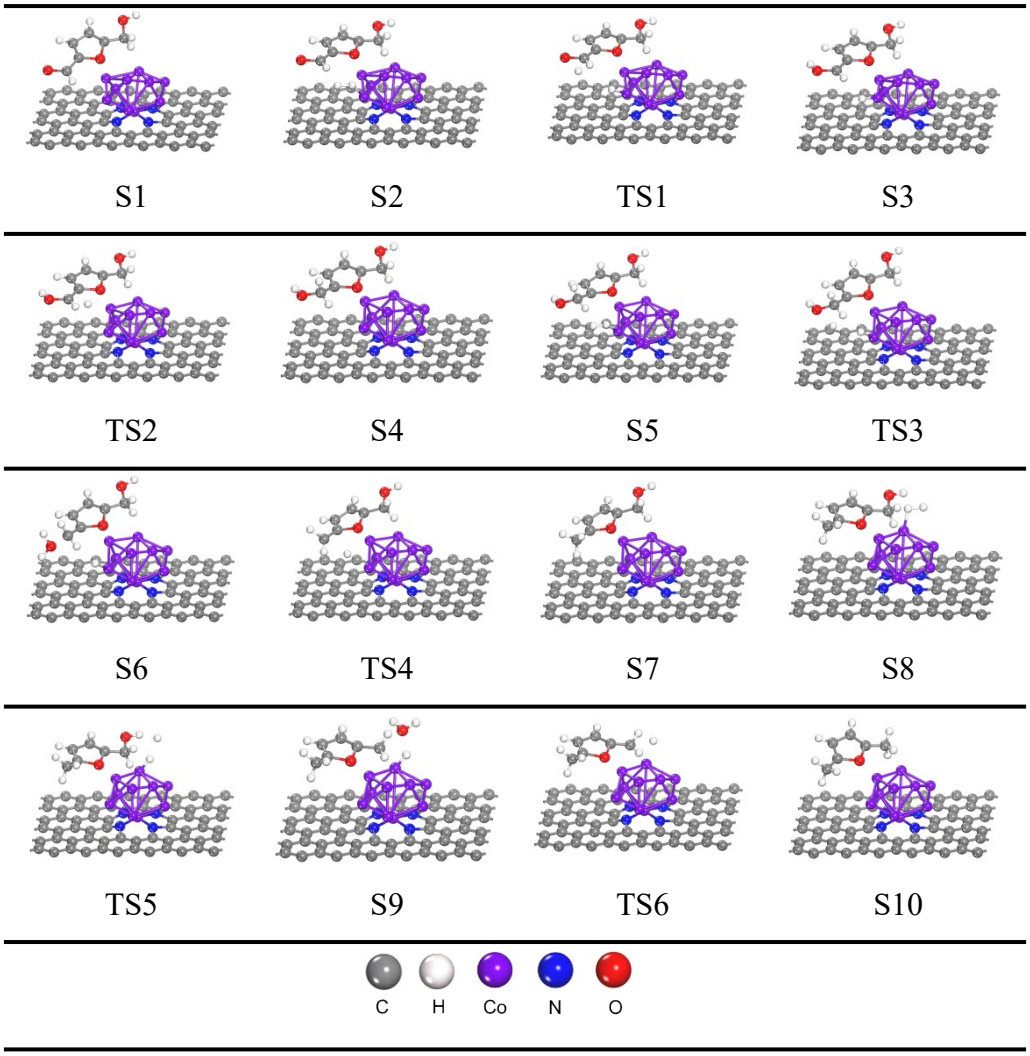

Figure S10. Compositions and geometries of the series of the intermediate states (S1-S10), and the series of the transition states (TS1-TS6) in the hydrogenation reaction of HMF over Co_n-NPs sites.

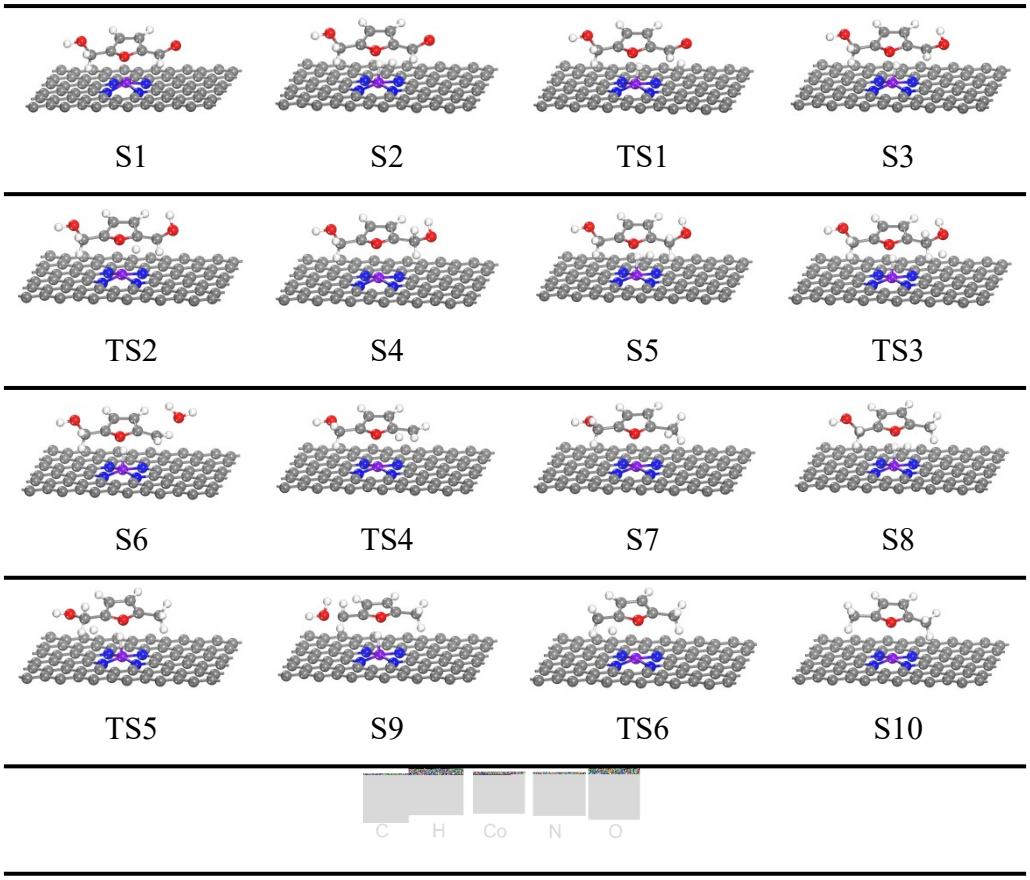

Figure S11. Compositions and geometries of the series of the intermediate states (S1-S10), and the series of the transition states (TS1-TS6) in the hydrogenation reaction of HMF over CoN_4 sites.

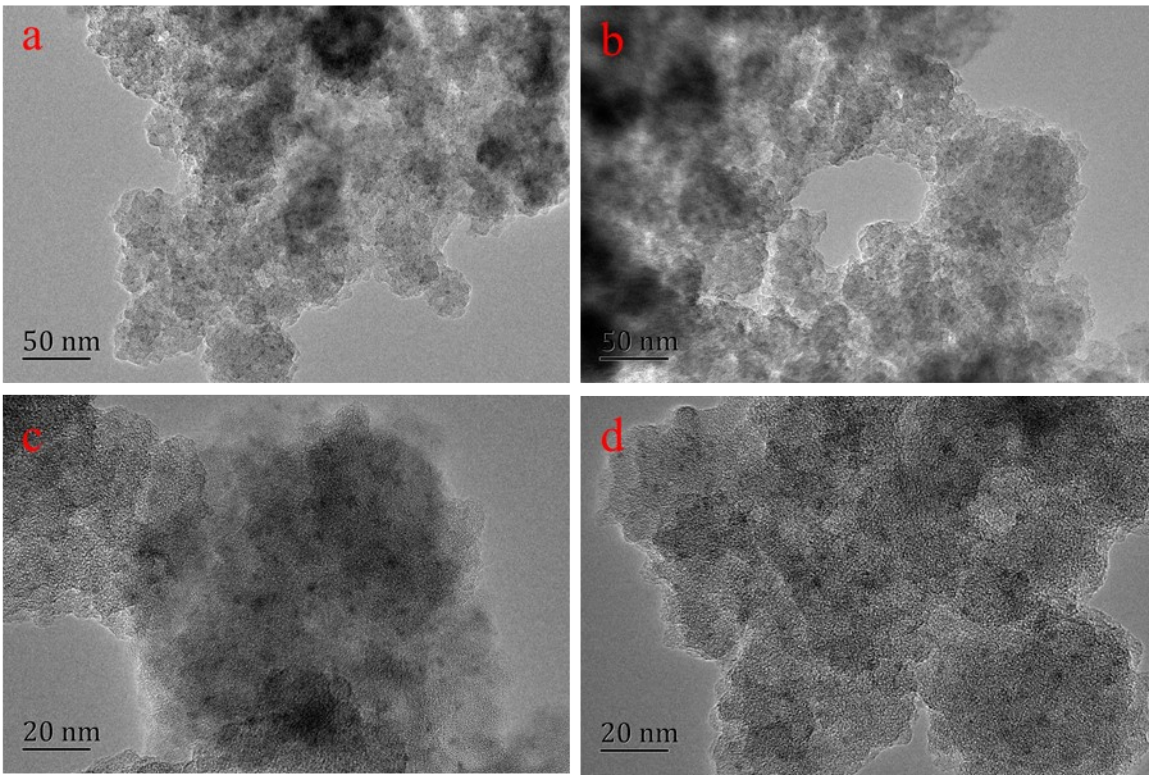

Figure S12. The TEM images of Co-N/C-450.

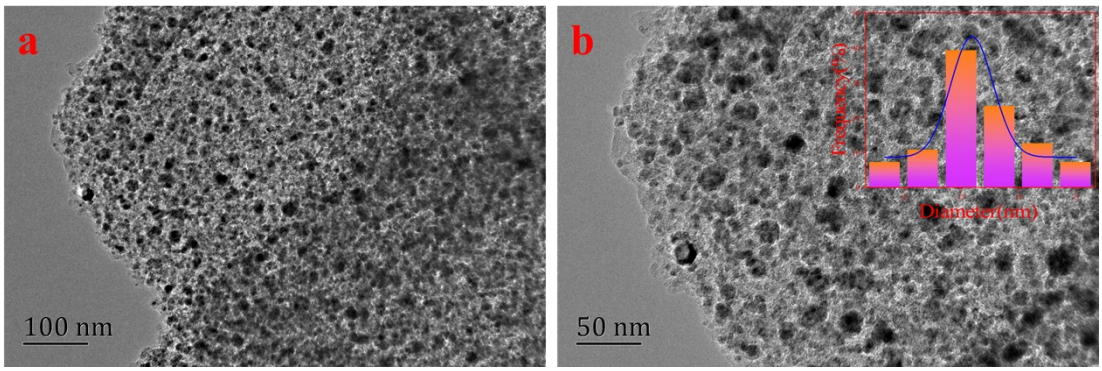

Figure S13. The TEM images of Co-N/C-600.

Table S1. ICP-OES data of Co-N/C-400 and Co-N/C-500 samples.

Sample	Co Loading (%)
Co-N/C-400	2.23
Co-N/C-500	3.35

Table S2. Fitting parameters at the Co K-edge for various samples (S_0^2=0.75).

Sample	Shell	N^a	R(Å)^b	$\sigma^2\times10^3$(Å^2)^c	ΔE_0 (eV)^d	R factor
Co foil	Co-Co	12*	2.49±0.01	6.4±0.1	8.3±0.2	0.001
CoO	Co-O	6.1±1.1	2.11±0.02	8.2±2.4	-0.9±2.7	0.006
	Co-Co	12.4±1.5	3.01±0.01	8.6±1.3	-3.1±1.3	
Co-N/C-400	Co-N/O	5.3±1.0	1.98±0.01	9.2±2.5	-5.0±2.1	0.016
Co-N/C-500	Co-N/O	3.5±0.6	1.99±0.01	9.8±2.1	-0.1±1.7	0.006
	Co-Co	4.5±0.8	2.92±0.01	10.2±1.5	-6.7±1.6	

[a]N: coordination numbers; [b]R: bond distance; [c]σ^2: Debye-Waller factors; [d] ΔE_0: the inner potential correction. R factor: goodness of fit.